A common mechanism links activities of butyrate in the colon

Mohit S. Verma[1,§], Michael J. Fink[1,§], Gabriel L. Salmon[1], Nadine Fornelos[2], Takahiro E. Ohara[3], Stacy H. Ryu[3], Hera Vlamakis[2,4], Ramnik J. Xavier[2,5*], Thaddeus S. Stappenbeck[3*], and George M. Whitesides[1,6,7*]

[1]Department of Chemistry and Chemical Biology, Harvard University, 12 Oxford Street, Cambridge, MA 02138, USA.

[2]The Broad Institute of MIT and Harvard, Cambridge, MA 02142, USA.

[3]Department of Pathology and Immunology, Washington University School of Medicine, St. Louis, MO 63110, USA

[4]Department of Microbiology and Immunobiology, Harvard Medical School, Boston, MA 02115, USA.

[5]Center for Computational and Integrative Biology and Gastrointestinal Unit, Massachusetts General Hospital, Harvard Medical School, Boston, MA 02114, USA.

[6]Wyss Institute for Biologically Inspired Engineering, Harvard University, 60 Oxford Street, Cambridge, MA 02138, USA.

[7]Kavli Institute for Bionano Science and Technology, Harvard University, 29 Oxford Street, Cambridge, MA 02138, USA.

[§]These authors contributed equally.

Abstract

Two biological activities of butyrate in the colon (suppression of proliferation of colonic epithelial stem cells and inflammation) correlate with inhibition of histone deacetylases. Cellular and biochemical studies of molecules similar in structure to butyrate, but different in molecular details (functional groups, chain-length, deuteration, oxidation level, fluorination, or degree of unsaturation) demonstrated that these activities were sensitive to molecular structure, and were compatible with the hypothesis that butyrate acts by binding to the Zn^{2+} in the catalytic site of histone deacetylases. Structure-activity relationships drawn from a set of 36 compounds offer a starting point for the design of new compounds targeting the inhibition of histone deacetylases. The observation that butyrate was more potent than other short-chain fatty acids is compatible with the hypothesis that crypts evolved (at least in part), to separate stem cells at the base of crypts from butyrate produced by commensal bacteria.

The epithelium of the mammalian colon is an important site for host-microbe interactions[1]. Among other activities, these microbes produce short-chain fatty acids (SCFAs)—mainly acetate, propionate, and butyrate—by anaerobic fermentation of dietary fiber. Butyrate, in particular, serves as the predominant source of energy for colonic epithelial cells under respiratory (oxidative) metabolism, even in the presence of another carbon source (glucose[2]). In addition, butyrate has been proposed to have two other effects in the colon: i) to promote anti-inflammatory activities in macrophages present in the *lamina propria* of the colon (e.g., through suppression of production of interleukin-6 (IL-6)[3]), and ii) to suppress the proliferation of colonic epithelial stem cells (CESCs), which are present at the base of colonic crypts[4]. These observations led Stappenbeck *et al*.[4] to propose that colonic crypts *co-evolved* with the gut microbiota to separate stem cells from microbiota-derived metabolites under healthy conditions. The mechanism by which these homeostatic conditions are maintained is not fully understood. In addition, it is unclear whether all effects of butyrate are beneficial.

This study uses a physical-organic approach[5] to show that a shared biochemical mechanism (inhibition of the activity of histone deacetylases[4, 6, 7] (HDACs)) underlies two of the observed physiological activities of butyrate: i) the suppression of production of IL-6 by macrophages (which is commonly interpreted as a *beneficial* effect under conditions of *normal health*[3, 6-8]), and ii) the suppression of proliferation of stem cells. (This suppression of proliferation is ambiguous in its benefits to the host.[4]) Our experimental design interprets trends in biological activity in terms of incremental variations in molecular structure, and is thereby largely insensitive to systematic errors in experiments that make difficult the interpretation of individual or sparse sets of biological data. We also confirm that butyrate is the strongest inhibitor of the activity of HDACs, among the SCFAs.

Histones are responsible for the packing of DNA as chromatin[9] within the nucleus of eukaryotic cells. Lysine amino groups on histones provide positive charges that mediate the electrostatic attraction between histones and the negatively charged backbone of DNA. Acetylation of lysine residues—a major posttranslational modification for histones[10-12]—neutralizes the positive charge and relaxes the chromatin structure. Deacetylation of the acetylated lysine residues on histones condenses the chromatin, which correlates with reduced transcription of genes[9].

HDACs are the catalytic core of the complexes of proteins involved in the modification of chromatin and suppression of gene expression[13]. The roles of these complexes vary from one cell type to another[13]: i) in CESCs, the action of HDACs maintains proliferation by decreasing the access of the transcription factor Foxo3 to its target genes[4]; ii) in intestinal macrophages (the most abundant mononuclear phagocytes in the *lamina propria*), the activity of HDACs upregulates the pro-inflammatory genes *Il6, Nos2, Il12a,* and *Il12b*.[3] The CESCs are responsible for the renewal of the intestinal epithelium[4], whereas the macrophages are a major contributor to innate immune responses and homeostasis in the presence of commensal microbes[3].

Riggs *et al.*[14] proposed that butyrate was an inhibitor of HDACs. They observed that addition of butyrate to a mammalian cell culture increased the presence of acetylated histones (in HeLa cells, initially, acetylated fractions of the H4 histones were undetectable, but after exposure to 3 mM butyrate for 24 h, acetylated fractions comprised 80% of the H4 histones[14]).

Two plausible mechanisms have been proposed for the observation of increased acetylation: i) inhibition of the activity of HDACs, or ii) activation of G-protein-coupled receptors (GPCRs), which reduces the expression of HDAC-encoding genes[15].

One study[16] reported that activities of other SCFAs as inhibitors of HDAC are lower than that of butyrate (the % inhibition of HDACs I and II from calf thymus, as measured by the release of [^{3}H]acetate from radioactively labelled acetylated histone, followed this order when tested at 0.25 mM: acetate (10%), propionate (60%), butyrate (80%), pentanoate (60%), and hexanoate (30%)[16]). Another study[17] reported that for the inhibition of HDACs present in nuclear extracts of HeLa cell lines (determined using a colorimetric HDAC assay kit), other SCFAs showed effects comparable to that of butyrate (1 mM propionate, butyrate, and pentanoate all showed approximately 80% inhibition[17]). The concentration of butyrate in the lumen is sufficiently high (~ 20 mmol/kg of wet feces[18]) to inhibit the activity of HDACs even if the inhibitory concentration (IC_{50}) is in the high micromolar to low millimolar range.

Although these observations strongly suggest a relationship between the presence of butyrate and the inhibition of HDACs, two unanswered questions remain: i) Are the physiological activities of butyrate (suppression of inflammation and proliferation) due to the inhibition of the activity of HDACs? ii) Is the interaction between butyrate and HDACs specific to the molecular structure of the short-chain fatty acid (i.e. an alkyl chain of a specific length *and* a carboxylate group)?

Here, we have examined molecules that are analogs of butyrate to understand which components of structure are relevant for its activity, and to establish compatibility or incompatibility of these relationships with hypotheses relating molecular structure to biological function. This paper tests three hypotheses (Table 1) postulated to explain the link between the non-respiratory physiological activities of butyrate, in particular, decreased production of IL-6 by bone-marrow-derived macrophages (BMDMs) and reduced proliferation of CESCs.

Table 1: Hypotheses addressing the biological activity of butyrate and assays to test the hypotheses.

	Hypothesis	Assay	Molecules to test (Supplementary Table S1)	Test
A	Butyrate suppresses the proliferation of CESCs and the expression of IL-6 in BMDMs by inhibiting the activity of HDACs.	• Activity of HDACs • Proliferation of CESCs • Expression of IL-6 in BMDMs	**1-12**	If results from the inhibition of HDACs do not correlate with the suppression of proliferation of CESCs and the expression of IL-6 in BMDMs, then hypothesis **A** is false.
A.1	Butyrate inhibits HDACs by binding to Zn^{2+} in the catalytic site.	• Activity of HDACs	**1-36**	If there is no correlation between the affinity of the metal-binding group towards Zn^{2+} and the inhibition of activity of HDACs, then hypothesis **A.1** is false.
B	Butyrate is not the most active species, but oxidative products of butyrate, or other low molecular-weight acids (either metabolites or different carbon structures), are more important regulators of the biological activity (i.e. suppression of proliferation of CESCs and suppression of expression of IL-6 in BMDMs).	• Proliferation of CESCs • Expression of IL-6 in BMDMs	**1-12**	If oxidative metabolites or other low molecular-weight acids show lower activity (i.e. the suppression of proliferation of CESCs and expression of IL-6 in BMDMs) than butyrate, then hypothesis **B** is false.

CESCs: colonic epithelial stem cells, IL-6: interleukin-6, BMDMs: bone-marrow derived macrophages, HDACs: histone deacetylases, SCFAs: short-chain fatty acids.

The experimental design and methods are detailed in the Online Methods. Here we sketch their features. To assemble data either compatible or incompatible with the hypotheses listed in Table 1, we selected analogs of butyrate (Table 2): similar molecules that vary either by chain length, functional group, branching, degree of unsaturation, and/or replacement of groups (CH_2 by S; H by F or D). We also examined molecules that are oxidative products of butyrate[19]. We used three types of assays: i) a cell-free assay for the activity of HDACs based on the enzymatic conversion of a fluorescent substrate[20] (Scheme 1), ii) a cellular assay that measures the proliferation of CESCs, and iii) immunoassays for measuring cytokines (IL-6, IL-10, TNFα—Figure 1 and Supplementary Figure S1) produced by BMDMs.

Table 2: Groups describing the selection of compounds for testing hypotheses.

Group	Compounds	Description
1	**1-5**	Short-chain fatty acids, including butyrate.
2	**6-12**	• Oxidative metabolites of butyrate by β-oxidation: in order of increasing oxidation level: a double bond at C2, alcohol substituent at C3, or a ketone at C3 (predominantly present as the enol tautomer). • Compounds resulting from ω-oxidation of butyrate or of 2-butenoate (alcohol substituent at C4) • Partially or completely deuterated forms of butyrate. These compounds have been reported to show kinetic isotope effects (ratio of the second order rate constants k_{HH}/k_{DD} is reported to be between 5.7 and 7.0[21]) in oxidative metabolism.
3	**13-21**	• Analogs of butyrate ($CH_3CH_2CH_2X$) where X is a functional group (carboxylate, hydroxamic acid, amide, sulfonate, or sulfonamide). This group also includes analogs that vary the basicity of the carboxylate in butyrate. (See Supplementary Table S1 for relevant pK_a values.) • A small group of hydroxamic acids (**13-16**) with different chain lengths. We expect hydroxamic acids to bind to Zn^{2+} more strongly than carboxylates.
4	**8-12, 22-36**	This group is designed to establish the relative activity of analogs of butyrate that differ in three ways: i) in their flexibility and conformation (as a result of double or triple bonds at either C2 or C3), ii) in their electronic structure, without changing flexibility or conformation (by replacing C3 with sulfur), or iii) in shape, as a result of introducing branching (mono- or di-methyl-substitution) at C2 or C3.

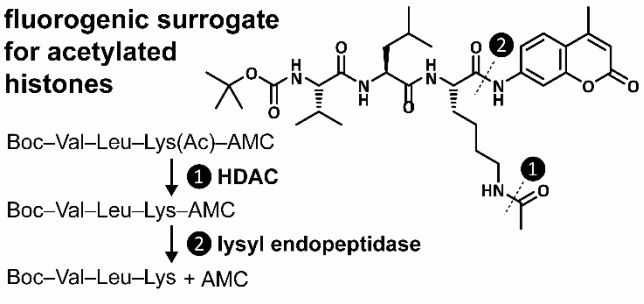

Scheme 1: Schematic illustration of the assay used for assessing activity of histone deacetylases (HDACs). The tripeptide conjugate of 7-amino-4-methylcoumarin (AMC) is used as a surrogate for lysine-acetylated histones[20]. Ac: acetyl, Lys: lysine, Leu: leucine, Val: valine, Boc: *tert*-butyloxycarbonyl.

Scheme 1 outlines the cell-free assay for the activity of HDACs[22]. The HDACs used in this assay are components of lysates of crude nuclear extracts from HeLa cells. Using this assay, we can assess the inhibition of activity of HDACs by analogs of butyrate without being limited by transport across the cell membrane and the nuclear membrane.

The cellular assay for proliferation of CESCs measures the mitotic activity of primary CESCs by recording levels of the cell-cycle phosphatase Cdc25A by luminescence[4]. The cells are harvested from knock-in mice expressing a fusion protein (a hybrid of Cdc25A and red luciferase from click beetle), and grown as rapidly dividing epithelial stem/progenitor cells[4]. *In vivo*, these cells are found at the base of intestinal crypts, and their proliferation influences the recovery of the epithelium from injury/inflammation[23]. Crypts have recently been suggested to have evolved in mammals to separate stem cells specifically from butyrate (and possibly other metabolites) produced by the microbiota[4]. If this suggestion is correct, we expect the potency of butyrate in suppressing the proliferation of CESCs to be higher than that of other SCFAs.

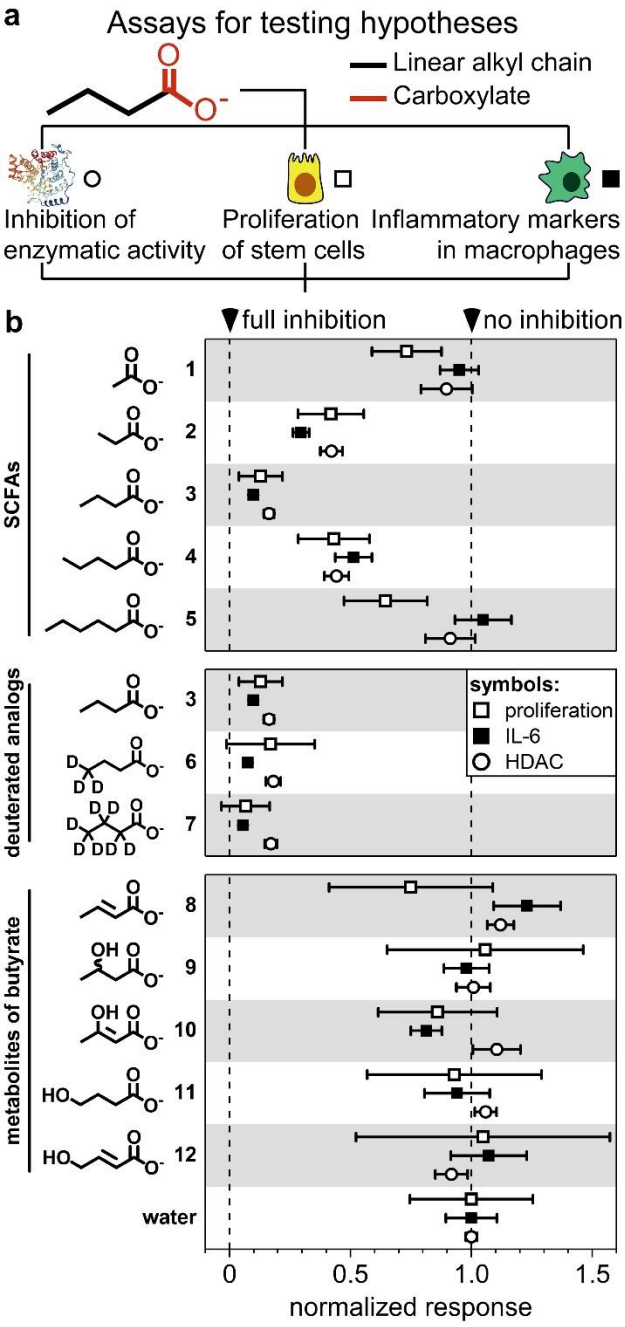

Figure 1: **The physiological activity of short-chain fatty acids depends on the chemical structure.** a) Schematic illustration of the assays used for testing butyrate and its analogs. b) Normalized response of analogs of butyrate from three different assays: proliferation of colonic epithelial stem cells (CESCs) (□), expression of interleukin-6 (IL-6) in bone-marrow-derived

macrophages (BMDMs) (■), and residual activity of histone deacetylases (HDACs, in a crude nuclear extract from HeLa cells) (○). All responses (in the form of either fluorescence, absorbance, or luminescence measurements) were first corrected to a blank sample (subtraction of background), and then normalized to unity using the value obtained with a solvent (i.e. water) sample (these samples do not receive a test inhibitor but instead only equivalent volume of water, which is the solvent used for the analogs of butyrate). The top section of the plot follows the change in chain length for SCFAs. The middle section of the plot shows that there is no kinetic isotope effect. The bottom section comprises possible oxidative metabolic products of butyrate. Data are reported as means. Error bars are 95% confidence intervals ($n \geq 7$). Supplementary Figure S4 shows values of individual datum for the HDAC assay, and sample sizes.

The assay involves incubating CESCs with butyrate and its analogs and monitoring the increase in luminescence over time; this increase corresponds to an increase in proliferation (Supplementary Figure S2). Effects of butyrate and it analogs on proliferation of CESCs are determined by normalizing the luminescence data to the initial values in each well (background) and the control sample (blank value obtained using an equivalent volume of water instead of a solution containing the test compound).

BMDMs are used as a model cell line for intestinal macrophages[3]. Measuring the production of cytokines by these cells indicates whether the analogs of butyrate are pro-inflammatory, or anti-inflammatory (these terms are context-dependent; here, we consider the role of macrophages in maintaining homeostasis in the presence of commensal microbiota, rather than during recovery from injury). We focus on the enzyme-linked immunoassay-based measurement of IL-6, which is a pro-inflammatory cytokine in most cells.[24] We measure IL-6 in the supernatants of cell cultures of BMDMs, when the cells are grown in the presence of butyrate and its analogs.

Inhibition of HDACs can downregulate the *Il6* gene[3]. We also report the production of IL-10 (an anti-inflammatory cytokine) and TNFα (a pro-inflammatory cytokine) in the supplementary information (Supplementary Figure S1).

We have examined 36 molecules (including butyrate) that are structurally similar to butyrate (Supplementary Table S1). We compare them as members of four groups (Table 2).

RESULTS

Inhibition of the activity of histone deacetylases correlates with the data from cellular assays

We tested butyrate and its analogs (Groups **1** and **2**, Table 2) using three independent assays: i) activity of HDACs (fluorescence); ii) proliferation of CESCs (luminescence); and iii) production of IL-6 by BMDMs (absorbance). The data obtained from each assay were baseline-corrected by subtracting values of the background noise, and then normalized to a control solvent sample (i.e., water; Figure 1A). The normalization allowed us to compare the effects of test molecules, using the three different assays, on proliferation of CESCs, production of IL-6 (and other proteins; Supplementary Figure S1) by BMDMs, and inhibition of the activity of HDACs (Figure 1B).

Although it is evident—from the analysis of SCFAs (compounds **1**-**5**), deuterated forms of butyrate (compounds **6**, **7**), and metabolites of butyrate (compounds **8**-**12**) in Figure 1B—that the results from the three different assays follow the same trends, we plotted the data from cellular assays against the inhibition of the activity of HDACs (Figure 2, compounds **1**-**12**) to visualize and quantify the correlation between them. This plot demonstrated that the physiological activities of analogs of butyrate (in CESCs and BMDMs) strongly correlate (slope = 1.03, R^2=0.87) with their potency in inhibition of the activity of HDACs in a cell-free assay (see

Supplementary Figure S3 for separated correlation plots of proliferation of CESCs, and expression of IL-6 in BMDMs). Thus, we cannot reject Hypothesis **A**.

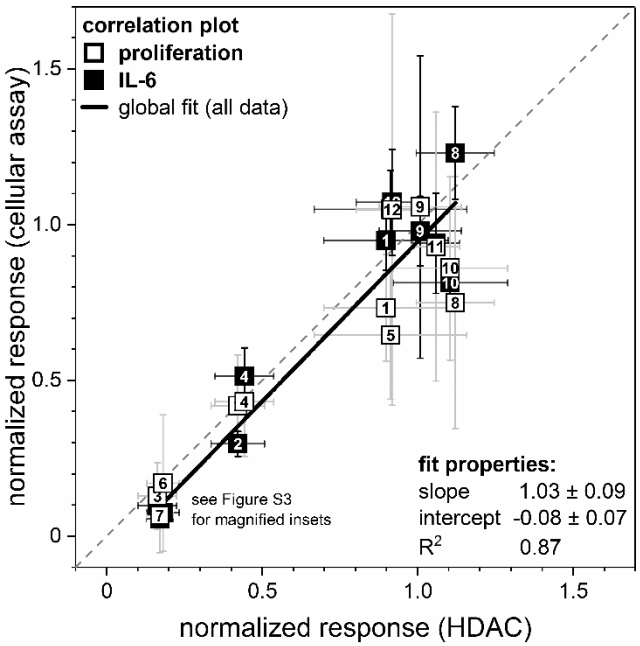

Figure 2: The physiological activities of butyrate correlate strongly with its inhibitory potency for HDACs. Normalized response from cellular assays plotted against the normalized response from the assay measuring activity of HDACs (same data as Figure 1B). Values are reported as mean ± S.D. ($n \geq 7$), and the identifying numbers for compounds are inscribed in the symbols. The dashed line represents the line $y = x$. The solid line is the linear fit of all data using Deming's maximum likelihood algorithm, which accounts for fitting error in both dimensions. All molecules were tested a 1 mM. The details of buffers used for each assay are in the Online Methods. See Supplementary Figure S3 for distinguishing overlapping points.

Oxidative products of butyrate are not responsible for the suppression of inflammation and proliferation

Figure 1B shows that butyrate was more potent at suppressing proliferation of CESCs and production of IL-6 by BMDMs than the other SCFAs and oxidative metabolites of butyrate. Thus, we reject Hypothesis **B**.

In addition, since the deuterated forms of butyrate have activities similar to butyrate (Figure 1B) and since oxidized metabolites of butyrate are less potent than butyrate, we conclude that products of oxidative transformation of butyrate do not play a role in its non-respiratory biological activities (although, of course, they could be intermediates in its role as a nutrient).

Butyrate is the optimal short-chain carboxylate to inhibit the activity of HDACs

Butyrate was the most active of the SCFAs in inhibition of HDACs (Figure 3; a concentration-dependent response for butyrate showed an IC_{50} of 0.17 ± 0.04 mM (n = 6)). The relationship between chain-length and activity was compatible with a shape-selective binding site that is optimal for butyrate. We also selected analogs of butyrate (Group **3**) where the functional group was varied in order to produce higher or lower expected affinity towards Zn^{2+} (which is present in the active site of HDACs). Within this group of analogs, for a constant chain length (four carbon or sulfur atoms; Figure 3), the molecule that we expected to bind most strongly to Zn^{2+} (compound **15**, with a hydroxamic acid functional group) produced the greatest inhibition of the activity of HDACs. The inhibitory potency decreased as the expected affinity toward Zn^{2+} decreased. These results are compatible with hypothesis **A**, and provide a mechanistic basis for it.

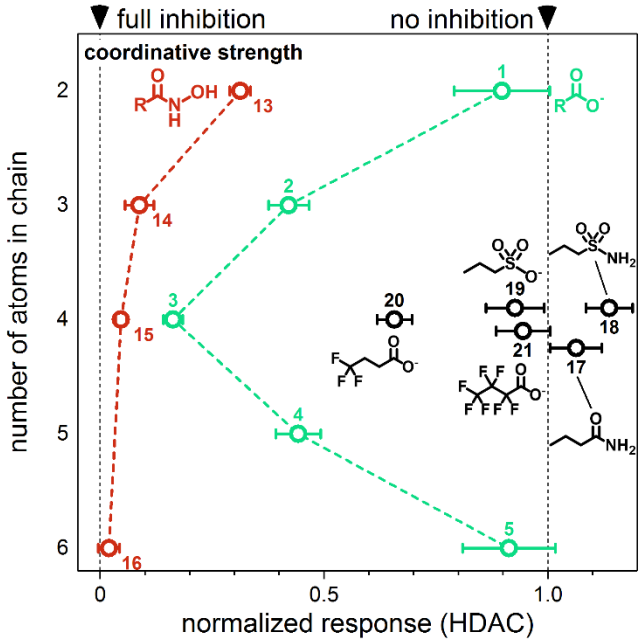

Figure 3: At a constant chain length (four carbon or sulfur atoms), functional groups with stronger expected affinity towards Zn^{2+} cause stronger inhibition of HDACs. Normalized response from the assay measuring the activity of HDACs in the presence of butyrate and its analogs. i) SCFAs (compounds **1-5**) that study the effect of varying the number of non-hydrogen atoms in the linear chain: R (and the number of atoms in the chain) is: methyl (2), ethyl (3), propyl (4), butyl (5), or pentyl (6)). ii) Hydroxamic acid analogs of the SCFAs (**13-16**). This functional group would bind to Zn^{2+} in HDAC. Identifying numbers for compounds are labelled next to the symbols. Data are reported as means. Error bars are 95% confidence intervals ($n \geq 8$). Values of individual datum, and sample sizes are shown in Supplementary Figure S4.

Four compounds $CH_3(CH_2)_{1\text{-}3,5}CONHOH$, with presumed strong affinity to Zn^{2+}, showed no local maximum in inhibition (Figure 3) at a concentration of 1 mM. (In comparison, at this concentration, the series $CH_3(CH_2)_{1\text{-}5}CO_2^-$ showed a local maximum in inhibition for butyrate.)

At chain lengths comparable to that of butyrate, the introduction of hydrogen bond donors or acceptors (alcohol or ketone groups), or a charged group (amines at physiological pH) resulted in lower inhibitory potency than butyrate (Figure 4). Only the relatively small changes in dipole induced by replacing CH_2 with S (CH_2 and S are similar by many measures) in position 3 (Figure 4, compound **24**) maintained some inhibitory potency.

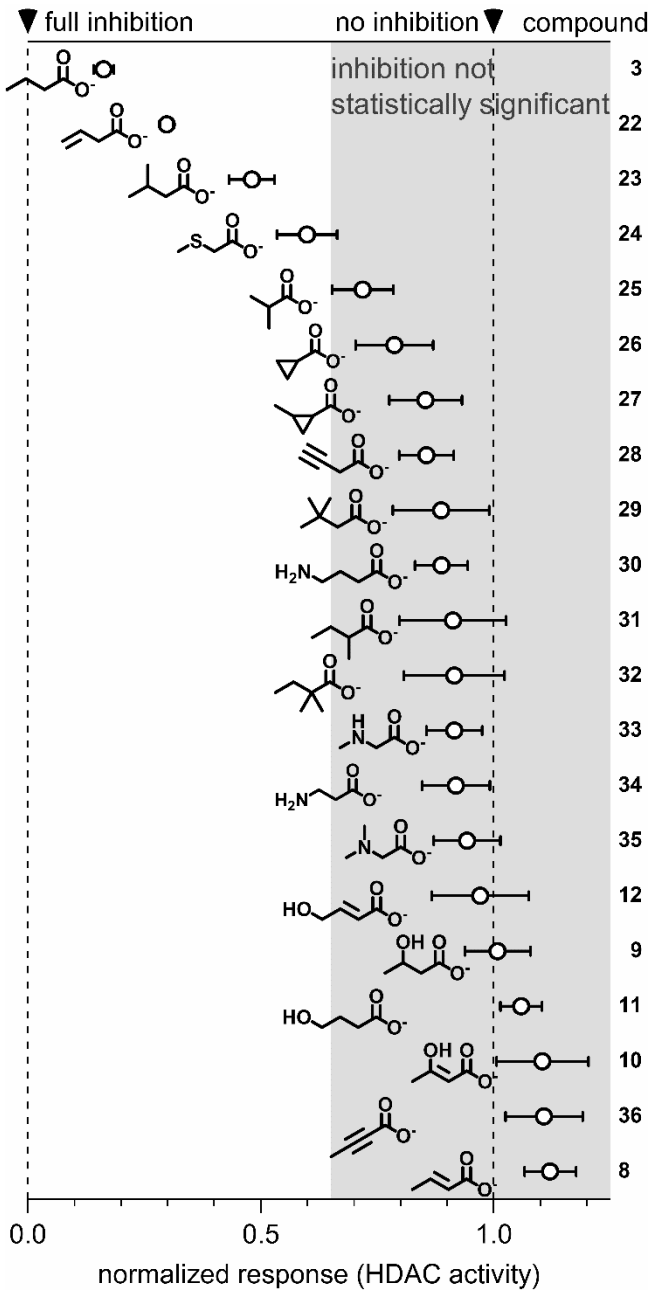

Figure 4: Flexibility and conformation of the analogs of butyrate determine inhibitory activity towards HDACs. Analogs of butyrate with modifications (e.g. addition of double or triple bonds, addition of branches, introduction of heteroatoms) to the alkyl backbone at C2, C3, or C4. Identifying numbers for compounds are provided on the right-hand axis. Data are reported as means. Error bars are 95% confidence intervals ($n \geq 8$). Values of individual datum, and sample sizes are shown in Supplementary Figure S4.

We conclude that the inhibition of HDACs combines selectivity in shape (linear butyrate) with selectivity for binding to Zn^{2+} (CONHOH or CO_2^-). These results are compatible with Hypothesis **A.1**, which provides a mechanistic explanation for Hypothesis **A,** which suggests that the physiological activities (suppression of proliferation of stem cells, and inflammation) of butyrate are due to its ability to inhibit HDACs.

DISCUSSION

We reject Hypothesis **B** (oxidative products of butyrate are important regulators of its biological activity), but do not reject Hypotheses **A** (butyrate acts by inhibiting HDACs) and **A.1** (butyrate inhibits HDACs by binding to Zn^{2+} in the catalytic site)**.** Thus our results are compatible with these hypotheses, but—as with many processes in complex biological systems—do not require them to be true.

Our examination of the biological activity of butyrate suggests that compounds that inhibit zinc amidases might provide approaches to inhibition of HDACs and modulation of their activity. These results suggest that *simple* molecules (e.g. butyrylhydroxamic acid, compound **15**) can provide high and relevant biological activity (e.g. inhibition of HDACs).

We demonstrate that inhibition of the activity of HDACs is the most plausible mechanism through which butyrate suppresses the proliferation of CESCs and the expression of IL-6 in BMDMs. The alternative mechanism of downregulating the expression of HDACs by activation of GPCRs is unlikely, because butyrate shows higher potency than other SCFAs in all three of the assays we used (Figure 1B), while butyrate is not selective in the activation of GPCRs (Supplementary Table S2[25]).

The importance of the activity of butyrate is context-dependent. In healthy individuals, when the structure of intestinal crypts is maintained, the concentration of butyrate that reaches the stem cells (which are at the base of the crypts) may plausibly be low (because rate of its mass transport is limited by diffusion, and because consumption of butyrate by cells at the surface of the crypts will also lower its concentration at the base of crypts). In these circumstances, butyrate is unlikely to have a marked effect on the stem cells in individuals with normal colonic function and health. The concentration of butyrate within the *lamina propria* close to the lumen could be high (in the mM range) because of the proximity to the microbiota and their metabolic products. Butyrate produced by the commensal microbiota could thus play a role in keeping the mobilizable cells such as macrophages in a regulated (non-inflammatory) state.

Upon injury or invasion by pathogens, the structural integrity of crypts is compromised, and the stem cells might be exposed to a higher concentration of butyrate than under healthy conditions. Their proliferation might thus be suppressed. The macrophages in the *lamina propria* would be exposed to a range of molecules produced by the microbiota and the host; some of these molecules might overcome the tolerogenic effects of butyrate and stimulate inflammation.

The high relative activity of butyrate among the SCFAs is compatible with (but does not demand) the proposal of Stappenbeck *et al*.[4] that anatomical features such as colonic crypts co-evolved in the colon together with butyrate-producing microbiota[4]. It is also compatible with the reverse (but potentially complementary) hypothesis: that this anatomical feature (perhaps evolved separately) might favor colonic bacteria that produce butyrate.

METHODS

Methods, materials, statistical analyses, and any associated references are available in the online version of the paper.

SUPPORTING INFORMATION.

Supplementary tables and figures are available in the supplementary information.

Acknowledgements

This work was funded by the Wyss Institute for Biologically Inspired Engineering, the Center for Microbiome Informatics and Therapeutics (Award # 6935953), the Crohn's & Colitis Foundation, and the Helmsley Charitable Trust. MSV was funded by a Banting Postdoctoral Fellowship (Code: 201409BAF-344359-257936) from the Government of Canada. MJF was funded by an Erwin Schrödinger Fellowship (grant no. J3771-N28) of the Austrian Science Fund (FWF). GLS was supported by the Wyss Institute for Biologically Inspired Engineering. NF, HV, and RJX are funded by the Crohn's and Colitis Foundation (Grant #20144126). We thank Daniel Graham, Caline Matar, and Thomas Sundberg for helpful discussions.

Author Contributions

MSV, MJF, and GMW designed the experiments. MSV, MJF, and GLS conducted experiments on the inhibition of activity of HDACs. NF conducted experiments on the expression of cytokines in BMDMs. TEO and SHR conducted experiments on the proliferation of CESCs. MSV, MJF, and GMW analyzed the data. HV, RJX, TSS, and GMW directed the research. MSV, MJF, and GMW prepared the manuscript with contributions and comments from all other authors.

Competing Financial Interests

The authors declare no competing financial interests.

References

1. Kaiko, G.E. & Stappenbeck, T.S. Host-microbe interactions shaping the gastrointestinal environment. *Trends Immunol* **35**, 538-548 (2014).
2. Roediger, W.E. Role of anaerobic bacteria in the metabolic welfare of the colonic mucosa in man. *Gut* **21**, 793-798 (1980).
3. Chang, P.V., Hao, L., Offermanns, S. & Medzhitov, R. The microbial metabolite butyrate regulates intestinal macrophage function via histone deacetylase inhibition. *Proc. Natl. Acad. Sci. U. S. A.* **111**, 2247-2252 (2014).
4. Kaiko, G.E. et al. The Colonic Crypt Protects Stem Cells from Microbiota-Derived Metabolites. *Cell* **165**, 1708-1720 (2016).
5. Whitesides, G.M. Physical-Organic Chemistry: A Swiss Army Knife. *Isr J Chem* **56**, 66-82 (2016).
6. Furusawa, Y. et al. Commensal microbe-derived butyrate induces the differentiation of colonic regulatory T cells. *Nature* **504**, 446-450 (2013).
7. Arpaia, N. et al. Metabolites produced by commensal bacteria promote peripheral regulatory T-cell generation. *Nature* **504**, 451-455 (2013).
8. Smith, P.M. et al. The microbial metabolites, short-chain fatty acids, regulate colonic Treg cell homeostasis. *Science* **341**, 569-573 (2013).
9. Kouzarides, T. Chromatin modifications and their function. *Cell* **128**, 693-705 (2007).
10. Yang, X.J. & Seto, E. Lysine acetylation: codified crosstalk with other posttranslational modifications. *Mol Cell* **31**, 449-461 (2008).
11. Zhao, S. et al. Regulation of cellular metabolism by protein lysine acetylation. *Science* **327**, 1000-1004 (2010).
12. Choudhary, C. et al. Lysine acetylation targets protein complexes and co-regulates major cellular functions. *Science* **325**, 834-840 (2009).
13. Bantscheff, M. et al. Chemoproteomics profiling of HDAC inhibitors reveals selective targeting of HDAC complexes. *Nat Biotechnol* **29**, 255-265 (2011).
14. Riggs, M.G., Whittaker, R.G., Neumann, J.R. & Ingram, V.M. n-Butyrate causes histone modification in HeLa and Friend erythroleukaemia cells. *Nature* **268**, 462-464 (1977).
15. Tan, J. et al. The role of short-chain fatty acids in health and disease. *Adv Immunol* **121**, 91-119 (2014).
16. Cousens, L.S., Gallwitz, D. & Alberts, B.M. Different accessibilities in chromatin to histone acetylase. *J Biol Chem* **254**, 1716-1723 (1979).
17. Gilbert, K.M., DeLoose, A., Valentine, J.L. & Fifer, E.K. Structure-activity relationship between carboxylic acids and T cell cycle blockade. *Life Sci* **78**, 2159-2165 (2006).
18. Topping, D.L. & Clifton, P.M. Short-chain fatty acids and human colonic function: roles of resistant starch and nonstarch polysaccharides. *Physiol Rev* **81**, 1031-1064 (2001).
19. Stumpf, P.K. Metabolism of Fatty Acids. *Annu Rev Biochem* **38**, 159-& (1969).
20. Tamai, K.M., Toshiaki; Wada, Emi; Tatsuzawa, Ayumi (ed. USPTO) (Cyclex Co., Ltd., United States; 2007).
21. Zielinska, A. & Zielinski, M. Deuterium kinetic isotope effect in the oxidation of deuteriated butyric acid-D-7 with chromium trioxide in 85% orthophosphoric acid. *J Radioanal Nucl Ch* **250**, 347-351 (2001).

22. Wegener, D., Wirsching, F., Riester, D. & Schwienhorst, A. A fluorogenic histone deacetylase assay well suited for high-throughput activity screening. *Chem Biol* **10**, 61-68 (2003).
23. van der Flier, L.G. & Clevers, H. Stem cells, self-renewal, and differentiation in the intestinal epithelium. *Annu Rev Physiol* **71**, 241-260 (2009).
24. Scheller, J., Chalaris, A., Schmidt-Arras, D. & Rose-John, S. The pro- and anti-inflammatory properties of the cytokine interleukin-6. *Biochim Biophys Acta* **1813**, 878-888 (2011).
25. Le Poul, E. et al. Functional characterization of human receptors for short chain fatty acids and their role in polymorphonuclear cell activation. *Journal of Biological Chemistry* **278**, 25481-25489 (2003).
26. Wilfong, E.M., Du, Y. & Toone, E.J. An enthalpic basis of additivity in biphenyl hydroxamic acid ligands for stromelysin-1. *Bioorg. Med. Chem. Lett.* **22**, 6521-6524 (2012).
27. AbdelHafez, E.M.N., Aly, O.M., Abuo-Rahma, G. & King, S.B. Lossen Rearrangements under Heck Reaction Conditions. *Adv Synth Catal* **356**, 3456-3464 (2014).
28. Sun, L. et al. Type I interferons link viral infection to enhanced epithelial turnover and repair. *Cell Host Microbe* **17**, 85-97 (2015).
29. Miyoshi, H. & Stappenbeck, T.S. In vitro expansion and genetic modification of gastrointestinal stem cells in spheroid culture. *Nat Protoc* **8**, 2471-2482 (2013).

ONLINE METHODS

Materials

Supplementary Table S1 lists the molecules tested in this work. All purchased molecules were specified to be >99% pure by the manufacturer. They were used without further purification and prepared as 100-mM stock solutions in water. Carboxylates with more than four carbon atoms were first deprotonated with an equimolar amount of aqueous 1 M NaOH and then diluted with water. Water was obtained from a Millipore purification system (resistivity > 18 MΩ.cm). HDAC activity assay kits (ab156064) were obtained from Abcam (Cambridge, MA, USA).

Synthesis

Hydroxamic acids **14** and **16** were synthesized by aminolysis of the methyl or ethyl esters using hydroxylamine, according to published procedure[26, 27]. The structural identity and purity were confirmed by nuclear magnetic resonance (NMR) spectroscopy; signals were in accordance with previously published values[26, 27].

Assay for inhibition of HDACs

The stock solutions were further diluted to 10 mM (to enable convenient and precise addition of volumes such that the final concentration would be 1 mM in the mixture used in the assay). The procedure for the assay was modified from manufacturer instructions by diluting the following reagents 4x in water: acetylated fluorescent tripeptide, deacetylated fluorescent tripeptide, crude nuclear extract, stop solution (containing trichostatin A (TSA)), and solution of lysyl endopeptidase. The volumes of these reagents used in the assay were increased 4x (compared to the manufacturer's protocol) to improve reproducibility (i.e. to obtain smaller errors from pipetting and mixing, by transferring volumes of at least 20 µL instead of only 5 µL as suggested

by the manufacturer). The recommended buffer was not changed (20 mM Tris-HCl, 125 mM NaCl, pH 8.0; supplied as 10x concentrate). The two-step method (the first step is deacetylation and the second step is cleavage of the fluorescent tag, Scheme 1) was used for assessing the activity of the molecules listed in Table 2. The following reagents were added to a well of the black 96-well plate: 120 µL of water, 20 µL of HDAC assay buffer, 20 µL of 4x diluted acetylated fluorescent tripeptide (i.e. Boc-Val-Leu-Lys(Ac)-AMC, Scheme 1[20]), 20 µL of test molecules (at a concentration of 10 mM in water), and 20 µL of 4x diluted HDACs (crude nuclear extract from HeLa cells). The 96-well microplate was placed on an orbital shaker at ~400 rpm for two minutes to mix the contents and then incubated at room temperature in the dark for 20 minutes. After incubation, 80 µL of 4x diluted stop solution was added to all the wells and the contents were mixed by placing the plate on the orbital shaker. Finally, 20 µL of 4x diluted developer (lysyl endopeptidase) was added to all the wells, the contents were mixed by shaking, and the plate was incubated at room temperature for 30-40 minutes before measuring the fluorescence at 450 nm (excitation 365 nm).

TSA (see Supplementary Table S1 for structure) at 1 µM final concentration in the assay was used as a known, strong inhibitor of HDACs. Water was used as a negative control (because it was the solvent for the test molecules). For each molecule that showed inhibition of HDACs, we performed an additional assay to check the influence on the developer by replacing the acetylated fluorescent tripeptide with deacetylated fluorescent tripeptide and eliminating HDACs from the mixture—this control confirms that the test molecule is not inhibiting the developer (lysyl endopeptidase). The fluorescence measurements from developer controls were higher by at least a factor of two than those obtained by the HDAC inhibition assay and hence, none of the test molecules meaningfully inhibited the developer.

Assay for proliferation of stem cells

Primary colonic epithelial cells were generated from Cdc25A-CBRLuc reporter mice and grown as three-dimensional spheroids in Matrigel as previously described[28]. Briefly, a small piece of the middle portion of the mouse colon was washed in sterile phosphate buffered saline (PBS) and digested in collagenase solution to isolate crypts. Isolated colonic crypts were plated in Matrigel (Corning) and cultured in 50% L-WRN conditioned media (50% CM) containing Wnt3a, R-spondin 3, and noggin (developed in-house) to enrich for epithelial stem/progenitor cells[29]. The 50% CM was further supplemented with 10 µM Y-27632 (ROCK inhibitor; R&D Systems). The resulting spheroids were passaged at least once before proceeding with the cell proliferation assay.

Three days after passaging and culturing in 50% CM, spheroids grown in Matrigel were scratched off the tissue-culture plate and resuspended in PBS-ethylenediaminetetraacetic acid (EDTA) solution (0.5 M EDTA in PBS). Spheroids were trypsinized for 2 minutes at 37 °C and dissociated into smaller homogenous fragments by vigorous pipetting up to 20-30 times. Cells were washed in 10% fetal bovine serum (FBS) in Dulbecco's Modified Eagle's Medium (DMEM)/F12, passed through a 40-µm cell strainer to remove larger fragments, and plated out in Matrigel in 96-well tissue culture plates, with each well containing 4 µL of the cell/Matrigel solution. A light microscope was used to ensure appropriate density (moderately dense) and fragment size (mostly single cells with a few small clumps) for the assay. Cells were then grown in 100 µl 50% CM for the first 24 hours, and then exchanged with media containing test molecules. Test molecules (at a final concentration of 1mM) or an equivalent volume of water were added to fresh 50% CM with 20 mM 4-(2-hydroxyethyl)-1-piperazineethanesulfonic acid (HEPES) and 150 µg/ml D-luciferin (Gold Bio). Addition of D-luciferin to Cdc25A-luciferase

expressing cells enabled a direct and live readout of mitotic activity over time. High-sensitivity luminescence readings were taken at 0, 16, 20, and 24 hours after addition of test molecules using the EnVision Plate Reader (PerkinElmer).

Assay for measuring cytokines in BMDMs

Murine bone marrow-derived macrophages (BMDMs) were differentiated from C57BL/6 bone marrow progenitors for 7 d in DMEM supplemented with 2 mM GlutaMAX, 10% (v/v) FBS, 100 U/mL penicillin-streptomycin, and 50 ng/mL mouse macrophage colony-stimulating factor (M-CSF). Differentiation efficiency was assessed by detection of cell surface markers CD11c (fluorescein isothiocyanate (FITC) anti-CD11c clone N418; eBioscience), CD11b (R-phycoerythrin anti-CD11b clone M1/70; eBioscience) and MHC class-II (Pacific blue anti-I-Ab clone AF6-120.1; BioLegend) using flow cytometry. BMDMs were seeded into 96-well tissue culture plates at 100,000 cells per well in 100 µL of complete DMEM, followed by incubation at 37 °C for 2 h to allow for adherence to plate. Butyric acid and analogs were added to generate a concentration of 1 mM per well (20 µL) in replicates of eight. Water was used as a negative control. Positive control for induction of IL-10 and inhibition of TNF-α was the salt-inducible kinase inhibitor HG-9-91-01 (500 nM). Positive control for the inhibition of IL-6 was TSA (25 nM). Thirty minutes after treatment with test molecules, cells were stimulated with lipopolysaccharide (LPS, 50 ng/mL final concentration). The supernatant was collected after 4 h and 16 h of incubation/stimulation for quantification of TNF-α, IL-6, and IL-10 using specific mouse enzyme-linked immunoassay (ELISA) sets (BD Biosciences). Cell viability was estimated by change in total cellular adenosine triphosphate (ATP) levels using CellTiter-Glo assays (Promega).

Data analysis and statistics

Assay for inhibition of HDACs

The fluorescence values obtained from the HDAC activity assays for each test molecule were corrected by subtracting the fluorescence obtained in wells containing TSA (as a potent inhibitor of HDAC). These TSA-corrected values were normalized by dividing by the fluorescence measurement obtained for the sample tested with water (without any inhibitor). As an additional control, 'blank' samples without any HDACs (but with all other components of the assay: fluoro-substrate peptide, buffer, stop solution, and developer) were used to check for background fluorescence. The mean values were calculated by combining normalized data from multiple experiments (and treating them as a single sample for each compound of interest, with sample sizes listed in Supplementary Figure S4) and calculating the average. The lower and upper limits of 95% confidence interval were calculated as:

$$\bar{x} - t_{1-\frac{\alpha}{2}}\left(\frac{s}{\sqrt{n}}\right)$$

$$\bar{x} + t_{1-\frac{\alpha}{2}}\left(\frac{s}{\sqrt{n}}\right)$$

where $\bar{x}$ is the mean, t is the t-value from Student's *t* distribution at desired significance level α (here 5%), *s* is the standard deviation of the sample, and *n* is the sample size (replicates from multiple experiments were combined and treated as a single sample with total sample sizes listed in Supplementary Figure S4). For each test compound, the 95% confidence interval is reported as error bars in the plots when comparison between data points is relevant (plotted using OriginLabs Origin® 2017).

In Figure 2, since a linear fit was obtained to determine correlation between normalized data, standard deviations were used as error bars to show the dispersion of the collected data.

In Figure 4, all the pairs of data (210 pairs) were first tested for statistical significance ($p < 0.05$) in the difference of their means using a one-way analysis of variance (ANOVA, Tukey test) to determine which pairs of data were significantly different from each other. (In one pair (isobutyrate vs. (methylsulfanyl)acetate), the Tukey test suggested that the pair was not significantly different, but when this pair was tested using Student's t-test, it was significantly different ($p<0.05$); these compounds were thus split into two separate groups.) The Tukey test allowed us to divide the entire dataset into two groups: one containing compounds, that do not significantly inhibit HDACs ($p > 0.05$) or that are not significantly different from the former ($p >0.05$), and another containing compounds that significantly inhibit HDACs ($p < 0.05$) and are significantly different from the first group. Finally, each datum in the second group was compared to the data in the first group (that does not inhibit HDAC significantly) as a whole (i.e. all data in this group were averaged together) using Student's t-test, and the resulting p-values were less than 0.001. Each datum in the second group was also compared to butyrate using the Student's t-test and the resulting p-values were less than 0.001.

Assay for proliferation of stem cells

The luminescence reading of the cells in the microplate were baseline-corrected by subtracting the data from wells that lacked D-luciferin (substrate of luciferase produced by the cells). The data were normalized to their respective initial times ($t = 0$ hr) by dividing by the initial baseline-corrected luminescence values. Finally, data are normalized to the relative increase in proliferation observed with the 'water' samples (these wells received water instead of a test molecule). The data obtained from the 16-h timepoints were used for analysis in Figure 1.

Assay for measuring cytokines in BMDMs

Absorbance values obtained from the readout of the ELISA were corrected for background signals, and then the concentrations (of TNF-α, IL-6, and IL-10) were calculated using a standard calibration curve. The concentrations were normalized to the value obtained from the 'water' samples (containing only water instead of the aqueous solution of the test compound).